

Unobtrusive Low Cost Pupil Size Measurements using Web cameras

Sergios Petridis, Theodoros Giannakopoulos and Costantine D. Spyropoulos
National Center for Scientific Research "Demokritos"

Unobtrusive every day health monitoring can be of important use for the elderly population. In particular, pupil size may be a valuable source of information, since, apart from pathological cases, it can reveal the emotional state, the fatigue and the ageing. To allow for unobtrusive monitoring to gain acceptance, one should seek for efficient methods of monitoring using common low-cost hardware. This paper describes a method for monitoring pupil sizes using a common web camera in real time. Our method works by first detecting the face and the eyes area. Subsequently, optimal iris and sclera location and radius, modelled as ellipses, are found using efficient filtering. Finally, the pupil center and radius is estimated by optimal filtering within the area of the iris. Experimental result show both the efficiency and the effectiveness of our approach.

Keywords: video analysis, eye tracking, pupil size estimation, physiological measurements

Motivation

Unobtrusive every day health monitoring can be of important use for the elderly population. In particular, pupil size may be a valuable source of information, since, apart from pathological cases, it can reveal the emotional state, the fatigue and the ageing. To allow for unobtrusive monitoring to gain acceptance, one should seek for efficient methods of monitoring using common low-cost hardware. A low cost camera that monitors the user while in front of a laptop or behind a mirror [Poh et al., 2011] falls into this scenario. Detecting pupils and pupil sizes in this context is of great importance. Namely, pupil sizes may be a valuable source of information, since, apart from pathological cases, it can reveal the emotional state [Partala and Surakka, 2003], the fatigue [Morad et al., 2000] and the ageing [Winn et al., 1994] of the subject under monitoring.

Towards this end, this work presents a method for detecting iris and pupils, including both their centers and sizes, from low resolution visible-spectrum images, using a robust unsupervised filter-based approach. Iris detection performance outperforms most state of the art methods compared, and is competitive to few others. With respect to pupil detection, to our knowledge, detecting pupil sizes detection is not reported elsewhere in the related literature. Using a dataset compiled in particular for this purpose, we show that our method is accurate enough to provide significant information for everyday long-term monitoring.

Relevant Work

The task of detecting eyes in images or videos is crucial and challenging in many computer vision applications. First, eye detection is a vital component of most face recognition systems, where eyes are used for feature

extraction, alignment, face normalization, etc.. In addition, eye tracking is widely used in human computer interaction (gaze tracking). Eye detection systems can be categorized according to the adopted data acquisition method in (a) visible imaging and (b) infrared imaging. According to the first [Jesorsky et al., 2001a, Zhou, 2004, Asteriadis et al., 2006, Hassaballah et al., 2011, Valenti and Gevers, 2008, Cristinacce et al., 2004, Hamouz et al., 2005], ambient light reflected from the eye area is captured, hence the task is rather difficult, due to the fact that captured information can contain multiple specular and diffuse components [Li, gram]. On the other hand, infrared-based approaches [Li, gram, Li et al., 2005, Villanueva et al., 2009] manage to eliminate specular reflections and lead to a better and accurate pupil detection. Another discrimination between eye detection approaches is based on the distance of the recording device: (a) head-mounted and (b) remote systems. Needless to say, head-mounted approaches can lead to more accurate systems. However, under particular requirements of low cost and low level of obstruction, remote sensing is the only acceptable solution.

Method

Preprocessing

The overall scheme of the proposed method is presented in Figure 1. At a first stage, the face is detected. Face detection is a well studied problem in machine vision [Viola and Jones, 2001] and there exist now several commercial tools that achieve high accuracy with high speed. For our purposes, we have used SHORE^{TM1} which achieves face

¹SHORETM:Sophisticated High-speed Object Recognition Engine, Fraunhofer IIS

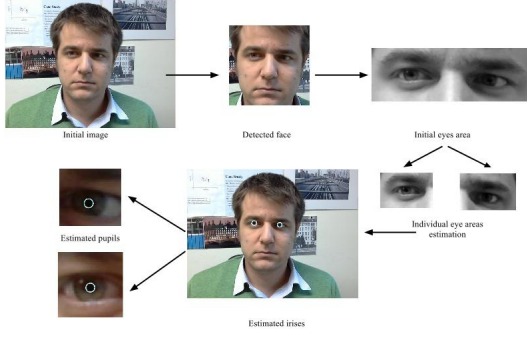


Figure 1. The overall architecture of the proposed method.

detection at a frame rate greater than 50fps.

The same engine, also provides directly as a rough estimate of the two eyes area, which we have used to initiate iris and pupil detection.



Figure 2. Sample eye area image

Sclera and Iris detection

The sclera/iris detection method aims at determining the coordinates $(e_x^L, E_y^L), (e_x^R, e_y^R)$ and the radii e_r^L, e_r^R of the left and right irises, considered as circular disks². Detection is done independently in each eye and is achieved by maximizing that output of a scoring process, while applying a specialized bank of linear filters parametrized by the radius of the iris, within the rough area of the eye. Therefore, this process results in both the estimation of the center of iris and its radius. The overall score is evaluated as a sum of three scores, based on luminosity, saturation and symmetry, whose definitions are given below.

Detection based on luminosity. Denoting the luminosity pixels of the eye rough area as I_L and the set of applied masks as $\{M_r^L\}$, the luminosity score is defined as:

$$l(e_x, e_y, e_r) = I_L[x, y, r] \cdot M_r^L \quad (1)$$

where \cdot above denotes element by element multiplication and $I_L[x, y, r]$ is the luminosity values of an image region centered at (x, y) and with size equal to the size of mask M_r^L .

The motivation here is that the iris can be located as a region *darker* than the surrounding sclera. To that end, we

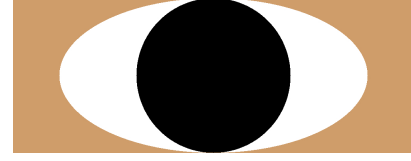


Figure 3. Mask for iris and sclera detection: The figure indicates with different shades the the three regions of the mask. The actual values depend on the criterion used and on the normalisation factor.

have used a mask with three regions, as depicted in Figure 3, where the elements of each region all share the same value. In particular:

iris a circle centered at the center of mask, where elements have the same *negative* value

sclera a region defined as the difference of the above circle and the co-centered ellipse of equal radius along the vertical axis and double radius along the horizontal axis, where elements have the same *positive* value

skin a region define as the difference of the above ellipse and a co-center rectangular region, where the elements have *zero* value

The mask values are normalized such that they sum up to zero.

Detection based on saturation. To detect the sclera and the iris, it is useful to observe that the sclera is typically much less saturated than both the iris and the surrounding skin. To that end we apply the same method as above using a set of masks M_r^S . These masks are similar to the ones used for detection based on luminosity, in that they are composed of the same regions. The difference lie in the value of pixel within each region. Namely, for the iris and skin elements share the same *positive* value whereas for the sclera the same *negative* value. As for luminosity, the mask values are normalized such that they sum up to zero. The score based on saturation is then evaluated as

$$s(e_x, e_y, e_r) = I_S[x, y, r] \cdot M_r^S \quad (2)$$

where I_S is the saturation values of the eye rough area considered.

Note that, as a practical approximation, our method actually uses the V channel of the YUV format to approximate saturation.

²The left (respectively right) eye is denoted by subscript L (respectively R)

Detection based on symmetry. A further observation to boost the accuracy of sclera and iris detection is that these regions show a significant symmetry. In particular, we have experimentally found that checking for horizontal symmetry inside the iris and sclera regions significantly removes false eye detections.

In particular, by denoting with superscript H an image region obtain by horizontal flipping, we evaluate the symmetry score as

$$h(e_x, e_y, e_r) = (|I_L[x, y, r] - I_L^H[x, y, r]| + |I_S[x, y, r] - I_S^H[x, y, r]|) \cdot M_r^H \quad (3)$$

Note that both luminance and saturation values are used here. The mask M_r^H is of similar structure to M_r^L , though with negative elements inside the sclera and iris and zero elements within the skin area.

Overall Score. The overall score for each candidate iris center and radius is evaluated as a sum over the respective luminance, saturation and symmetry scores.

$$c(e_x, e_y, e_r) = l(e_x, e_y, e_r) + s(e_x, e_y, e_r) + h(e_x, e_y, e_r) \quad (4)$$

and the final choice is made by exhaustively searching over the rough eye area found during preprocessing.

$$(\hat{e}_x, \hat{e}_y, \hat{e}_r) = \arg \max_{e_x, e_y, e_r} c(e_x, e_y, e_r) \quad (5)$$

Pupil Detection and measurement

As soon as the disk that defines the iris area for each eye has been estimated, the pupil is detected as a circle within the iris that optimal satisfies a gradient-based criterion. Candidate pupils are circles with center (p_x, p_y) in the close neighborhood of the iris center (e_x, e_y) , with radius such that they fall strictly inside the iris area.

The gradient criterion is evaluated as the difference between the average luminosity of the pixel defining the perimeter of the candidate circle with the average luminosity of the immediate outer pixels of the circle. The greater the difference, the greater the possibility that the circle corresponds to the pupil. Note that the sign of the difference is important here.

Though this approach is conceptually simple, it has shown that it is quite accurate, even in the presence of light reflections, which may degrade the performance of a non-gradient method.

Optimal Frame

The procedure outlined for detecting the iris and the pupil is repeated for every frame obtained from the camera, for both eyes. Since the ultimate goal is to measure the pupil size, and given that pupil size does not change from frame to frame³, it is not needed to measure the pupil on each frame,

but rather on a frame where it can be measured with higher confidence. To that end, we describe now a method that evaluates the optimal frame based on which detecting the pupil and measuring its size can be attempted.

Namely, for every frame, we compute an overall *confidence score*, as the product of the following measures:

- left eye iris detection score
- right eye iris detection score
- e_r^L and e_r^R equality based score
- e_y^L and e_y^R equality based score
- p_y^L and p_y^R equality based score

Regarding the first two items of the above list are directly given through Eq 4. The equality based scores are evaluated based on the generic formula

$$s = \frac{|l - r|}{\max\{l, r\}} \quad (6)$$

where l (respectively r) is a measured obtained from the left (respectively right) eye.

Therefore, as the video is streaming, we evaluate the overall confidence score and compare it to the one that has been obtained so far. In case it is greater, the less confident value is discarded and the new one is kept as the optimal one. In this way, the latest results are always based on the more confident frames. The procedure is repeated until the person under monitoring is stopped from being tracked, or after the end of a predefined time duration. In both case, the confidence score is reset and the procedure is repeated again.

Complexity Analysis

A main concern in the development of the proposed method has been to keep low the overall complexity. This has been important for two reasons. The first one relates to low resources that the method should be needing. Either running as a background process on a tablet, or as a process on a dedicated hardware, detecting and measuring pupils should take as few resources as possible, given that the same hardware may be hosting other processes too. The second one relates to the speed of execution. Even though pupil size measurement is not critical, and therefore latency is affordable, the need of video recording should nevertheless be avoided to address users' privacy concerns. Overall, our goal has been to measuring pupils in at least real time given limited processing resources and no storage.

One-pass iteration

The method that has been described in this paper does achieve this goal. In particular, a significant speed up has been achieved by allowing scores involving iterations over pixels to be computed with a single pass over the respective

³we assume here that lighting conditions stay the same

Method	E_l	E_r	E
HAAR	0.052	0.040	0.046
CART	0.060	0.057	0.058
Rough	0.054	0.053	0.053
Proposed	0.035	0.021	0.028

Table 1
Iris Detection Average Relative Error (left, right and overall) results (MATLAB-related methods compared)

Furthermore, we have compared our method against an tolerance-based accuracy measure widely used in the literature [Jesorsky et al., 2001a, Zhou, 2004, Asteriadis et al., 2006, Hassaballah et al., 2011, Valenti and Gevers, 2008, Cristinacce et al., 2004, Hamouz et al., 2005]. Namely, given an error tolerance T , an eye detection result is considered as successful if both errors e_l and e_r are less than T :

$$A_T = \frac{\sum_{i:\max(e_l(i), e_r(i)) \leq T} 1}{N} \quad (7)$$

Using this measure, it has been possible to compare the proposed method against [Jesorsky et al., 2001a, Zhou, 2004, Asteriadis et al., 2006, Hassaballah et al., 2011, Valenti and Gevers, 2008, Cristinacce et al., 2004, Hamouz et al., 2005] as well, using the corresponding reported results. A typical value for the threshold is $T = 0.25$, because it corresponds to an accuracy of about half the width of an eye in the image, while $T = 0.1$ has also been used [Zhou, 2004, Jesorsky et al., 2001b, Asteriadis et al., 2006]. In Table 2 the tolerance-based accuracy for three different tolerance thresholds is presented. The proposed method outperforms most of the compared methods, except for the case of $T = 0.05$.

Pupil size estimation performance

Pupils size estimation evaluation needs a different setting from the one described above. To begin with, annotations of the pupil's whole area, not just its center, is needed. To our knowledge, there is no available dataset with such annotations. Therefore, we have built a manually annotated dataset of pupil area. Three humans annotated the irises and pupils, to estimate an inter-annotator agreement level. Final pupil annotations have been considered as the average area of all annotators. The compiled dataset consists of 50 1280x960 resolution face images of 10 different humans.

With respect to the performance measures, we have used the recall, precision and F1 measures over the pupil areas. In particular, let A_a be the area of the manually annotated pupil, A_e be the area of the estimated pupil and A_c be the area of their intersection. The recall, precision and F_1 rates are defined as $R = \frac{A_c}{A_a}$, $P = \frac{A_c}{A_e}$ and $F_1 = \frac{2RP}{R+P}$ respectively.

Method	T		
	0.05	0.1	0.25
HAAR	22	75	98
CART	8	68	99
Rough	15	68	98
[Jesorsky et al., 2001a]	40	80	91
[Zhou, 2004]	-	-	95
[Asteriadis et al., 2006]	50	82	98
[Hassaballah et al., 2011]	45	85	95
[Valenti and Gevers, 2008]	84	91	99
[Cristinacce et al., 2004]	56	96	98
[Hamouz et al., 2005]	59	77	93
Proposed	47	92	99

Table 2
Iris detection tolerance-based accuracy results for three different tolerance values (all methods compared)

	Precision	Recall	F1
i-a.a	82	84	79
Proposed Method	66	68	67

Table 3
Pupil detection performance and comparison to inter-annotator agreement (i-a.a).

These same measures have also been used for evaluating the inter-annotator agreement. The results of the evaluation are displayed in Table 3. Note that the inter-annotation agreement scores are relatively low, revealing the difficulty even for a human in annotating the pupil area, especially for dark and brown eyes.

In terms of average F_1 measure, the proposed pupil detection method is 12% less accurate than the human annotation performance. In terms of pupil diameter size estimation, our method achieves on average 85% accuracy. This means that for an average 6mm pupil diameter, average error is 0.9mm, which is much lower than the threshold of 2mm indicated for significant pupil differentiations [Partala and Surakka, 2003, Winn et al., 1994].

A specific benchmark dataset containing such cases would nevertheless be needed to explicitly verify this conclusion.

Discussion

A method for iris and pupil detection, including their sizes, has been presented, based on a robust unsupervised recursive filtering technique. Evaluation on iris center detection has shown that the proposed method outperforms most of related algorithms. Pupil size estimation was evaluated on a separate dataset which also contains annotations regard-

ing not only pupils position but their sizes as well. The final pupil detection performance results showed that the proposed method's accuracy is accurate enough to be considered as a low cost pupillometry for long-term monitoring. Further results on video should be presented to show the utility of the confidence of the result based on frame sequences.

Acknowledgments

The research leading to these results has been funded by the European Union's Seventh Framework Programme (FP7/2007-2013) under grant agreement no 288532. For more details, please see <http://www.usefil.eu>.

References

- [Asteriadis et al., 2006] Asteriadis, S., Nikolaidis, N., Hajdu, A., and Pitas, I. (2006). An eye detection algorithm using pixel to edge information. In *European Signal Processing Conf. (EUSIPCO)*.
- [Castrillón et al., 2007] Castrillón, M., D'Álmeida, O., Guerra, C., and Hernández, M. (2007). Encara2: Real-time detection of multiple faces at different resolutions in video streams. *J. Visual Communication and Image Representation*, 18(2):130–140.
- [Cristinacce et al., 2004] Cristinacce, D., Cootes, T., and Scott, I. (2004). A multi-stage approach to facial feature detection. In *BMVC*, pages 231–240.
- [Hamouz et al., 2005] Hamouz, M., Kittler, J., Kamarainen, J.-K., Paalanen, P., Kalviainen, H., and Matas, J. (2005). Feature-based affine-invariant localization of faces. *Pattern Analysis and Machine Intelligence, IEEE Transactions on*, 27(9):1490–1495.
- [Hassaballah et al., 2011] Hassaballah, M., Murakami, K., and Ido, S. (2011). An automatic eye detection method for gray intensity facial images. *International Journal of Computer Science*, 8.
- [Jesorsky et al., 2001a] Jesorsky, O., Kirchberg, K., and Frischholz, R. (2001a). Robust face detection using the hausdorff distance. In *Audio-and video-based biometric person authentication*, pages 90–95. Springer.
- [Jesorsky et al., 2001b] Jesorsky, O., Kirchberg, K., and Frischholz, R. (2001b). Robust face detection using the hausdorff distance. In *Audio-and video-based biometric person authentication*, pages 90–95. Springer.
- [Li, gram] Li, D. (Iowa State University Human Computer Interaction Program.). Low-cost eye-tracking for human computer interaction. Master's thesis, 2006.
- [Li et al., 2005] Li, D., Winfield, D., and Parkhurst, D. J. (2005). Starburst: A hybrid algorithm for video-based eye tracking combining feature-based and model-based approaches. In *Proceedings of the IEEE Computer Society Conference on Computer Vision and Pattern Recognition*.
- [Morad et al., 2000] Morad, Y., Lemberg, H., Yofe, N., and Dagan, Y. (2000). Pupillography as an objective indicator of fatigue. *Current Eye Research*, 21(1):535–542.
- [Partala and Surakka, 2003] Partala, T. and Surakka, V. (2003). Pupil size variation as an indication of affective processing. *International Journal of Human-Computer Studies*, 59(1–2):185 – 198. <ce:title>Applications of Affective Computing in Human-Computer Interaction</ce:title>.
- [Poh et al., 2011] Poh, M., McDuff, D., and Picard, R. (2011). A medical mirror for non-contact health monitoring. In *ACM SIGGRAPH 2011 Emerging Technologies*, page 2. ACM.
- [Shiqi,] Shiqi, Y. Eye detection. <http://yushiqi.cn/research/eyedetection>.
- [Valenti and Gevers, 2008] Valenti, R. and Gevers, T. (2008). Accurate eye center location and tracking using isophote curvature. In *Computer Vision and Pattern Recognition, 2008. CVPR 2008. IEEE Conference on*, pages 1–8. IEEE.
- [Villanueva et al., 2009] Villanueva, A., Daunys, G., Hansen, D., Böhme, M., Cabeza, R., Meyer, A., and Barth, E. (2009). A geometric approach to remote eye tracking. *Univers. Access Inf. Soc.*, 8(4):241–257.
- [Viola and Jones, 2001] Viola, P. and Jones, M. (2001). Rapid object detection using a boosted cascade of simple features. In *Computer Vision and Pattern Recognition, 2001. CVPR 2001. Proceedings of the 2001 IEEE Computer Society Conference on*, volume 1, pages I–511. IEEE.
- [Winn et al., 1994] Winn, B., Whitaker, D., Elliott, D., and Phillips, N. J. (1994). Factors affecting light-adapted pupil size in normal human subjects. *Investigative Ophthalmology & Visual Science*, 35(3):1132–1137.
- [Zhou, 2004] Zhou, Z. (2004). Projection functions for eye detection. *Pattern Recognition*, 37(5):1049–1056.